New Approaches for a Transparent Design of Multivariable Control Systems*

Herbert M. Schaedel
Rainer Bartz
Department of Information Technology, University of Applied Sciences Köln, Betzdorfer Strasse 2, 50679 Köln, Federal Republic of Germany

Multivariable control systems are of great importance in industry. The intention of this paper is to show a simple, effective and transparent method that can be applied to those problems without an unnecessary amount of mathematics. A binary distillation column and a fluid mixing process are taken as typical examples for multivariable processes with two inputs and two outputs. The multivariable controller is broken down into a decoupling block and a PI-controller block which is designed for the main branches of the decoupled process. Stationary and dynamic decoupling is discussed for two examples. The design procedure is a step by step design that can be interpreted in each phase. The decoupling block causes a paralleling of the main branches and the coupling branches of the original process. Therefore the problem arising from parallel effects in the decoupled branches is discussed in detail for three examples. The design can be done using just a pocket calculator. The individual design steps are made transparent by the CAE-tool SimTool in the time and frequency domain.

INTRODUCTION

Many industrial processes are multivariable processes where interrelationships cannot be neglected. Engineering education in control seems to ignore this fact. The design of a multivariable controller is rarely covered in detail during a basic lecture because the up to date procedures are far too complex and time consuming. So only engineers with a special education in control theory know how to treat such control circuits which are of great importance in industrial applications. The aim therefore is to present a didactic concept of multivariable controller design for basic control engineering education, providing engineers with a knowledge that can easily be applied in engineering practice.

In order to demonstrate the proposed technique we take a binary distillation column that has been referred to in literature several times to show modern design techniques, ie H_∞ and others. A second example refers to a typical flow mixing process with significant influence of delay times due to propagation of the fluid.

BINARY DISTILLATION COLUMN AS AN EXAMPLE FOR A MULTIVARIABLE CONTROL SYSTEM [1][2]

In chemical industries, distillation is one of the most important processes. Its objective is to separate a mixture of chemical components. The purpose of control is to maintain bottom and top product purity despite variations in feed flow and feed concentration up to $\pm 20\%$. Product purity is defined by the concentration of the high-boiling component in the bottom product and the concentration of the light-boiling component in the distillate. The plant to be controlled consists of 40 trays, a reboiler and a condenser (Figure 1). The mixture is continuously fed into tray 22. Trays 14 and 28 are amongst the most sensitive ones with respect to feed disturbances. Therefore the temperature sensors are placed on those trays. By keeping the tray temperatures T_{14} and T_{28} within a specified range around their steady-state val-
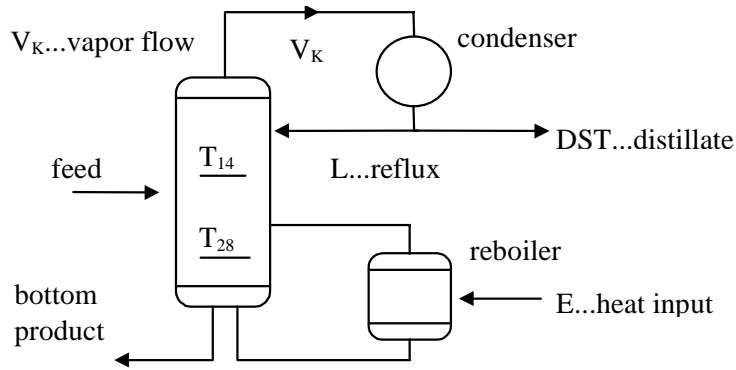
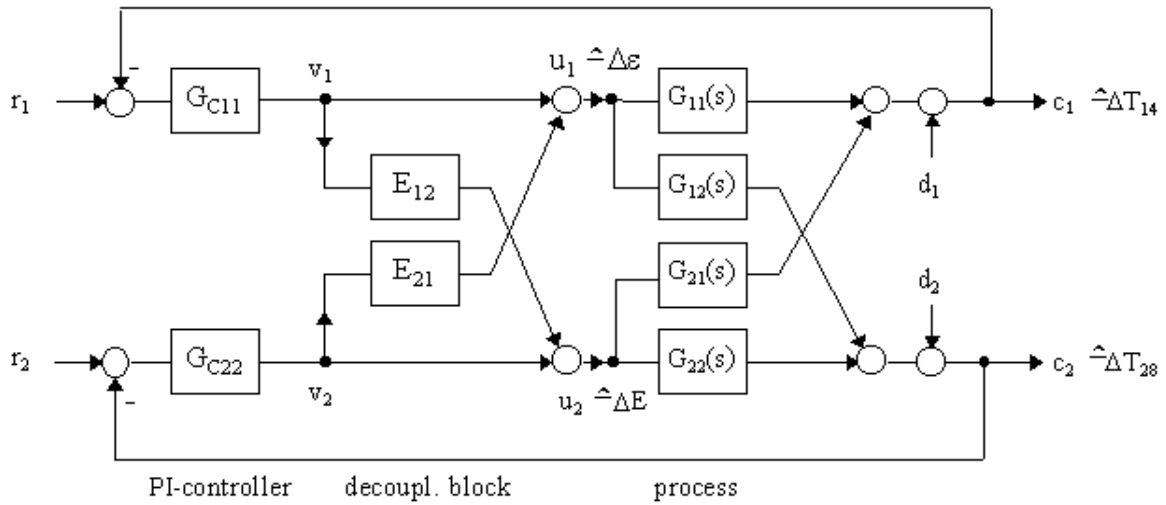Figure 1: Schematic representation of distillation column [1].

Figure 2: Block diagram of a multivariable control circuit with two inputs and two outputs.

ues, specifications for top and bottom product purity can be met. Therefore control of tray temperatures instead of concentrations is proposed. Concentration measurements are expensive and introduce additional time delays into the control loop.

Heat input E and reflux ratio $\varepsilon = L/V_k$ are chosen as manipulated variables. Δ means deviations from setpoint.

From step response to E and ε a simple linear input-output model is fitted. Time constants are given in hours.

$$\begin{bmatrix} \Delta T_{14} \\ \\ \Delta T_{28} \end{bmatrix} = \begin{bmatrix} G_{11}(s) & G_{21}(s) \\ \\ G_{12}(s) & G_{22}(s) \end{bmatrix} \begin{bmatrix} \Delta \varepsilon \\ \\ \Delta E \end{bmatrix} =$$

$$\begin{bmatrix} -\dfrac{1220}{1+6.1s} & \dfrac{100}{(1+1.2s)(1+1.5s)} \\ -\dfrac{1500}{1+2.7s} & \dfrac{324}{1+1.6s} \end{bmatrix} \begin{bmatrix} \Delta \varepsilon \\ \\ \Delta E \end{bmatrix} \qquad (1)$$

The changes in temperature T_{14} and T_{28} depend on both manipulated variables $\Delta \varepsilon$ and ΔE. Thus chang-

ing output variable T_{14} by the reflux ratio ε will also change output variable T_{28}.

The right part of Figure 2 shows the equivalent block diagram of the process with two inputs $\Delta \varepsilon$ and ΔE and two outputs ΔT_{14} and ΔT_{28}. Figures 3.1(a) and 3.2(a) show the step responses of the four branches of control. The p-canonical form for the process model is chosen for practical reasons in order to identify the model by simple input-output measurements. Changes of feed flow and concentration can be considered as disturbances at the plant outputs. The disturbance transfer function can be modelled as a second order lag:

$$G_d(s) = \frac{10}{(1+0.025s)^2} = \frac{d_i(s)}{D_i(s)} \qquad (2)$$

DESIGN OF A MULTIVARIABLE PI-CONTROLLER [4][8]

Figure 2 shows the whole block diagram of the control circuit. The controller is broken down into a decoupling block and a PI-controller block. In the first design step the decoupling block is evaluated for steady
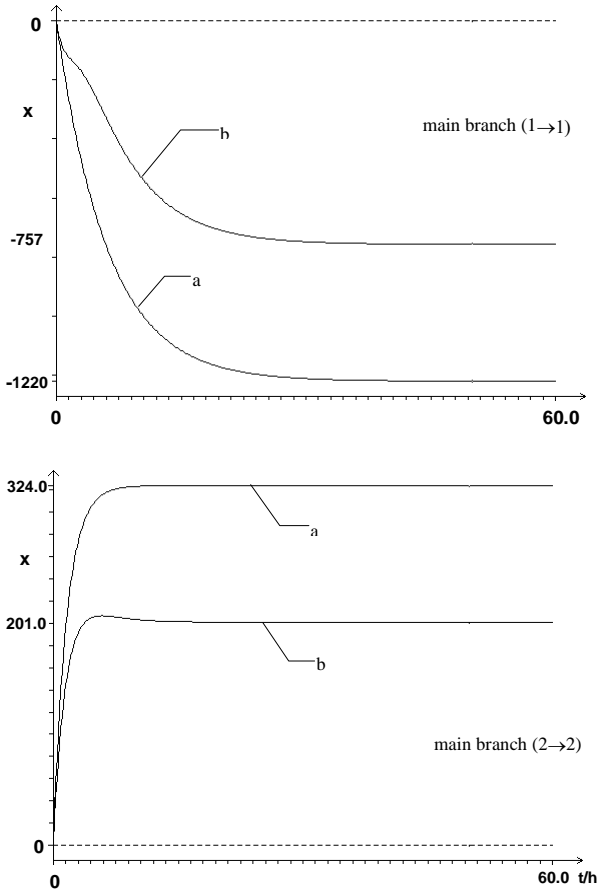
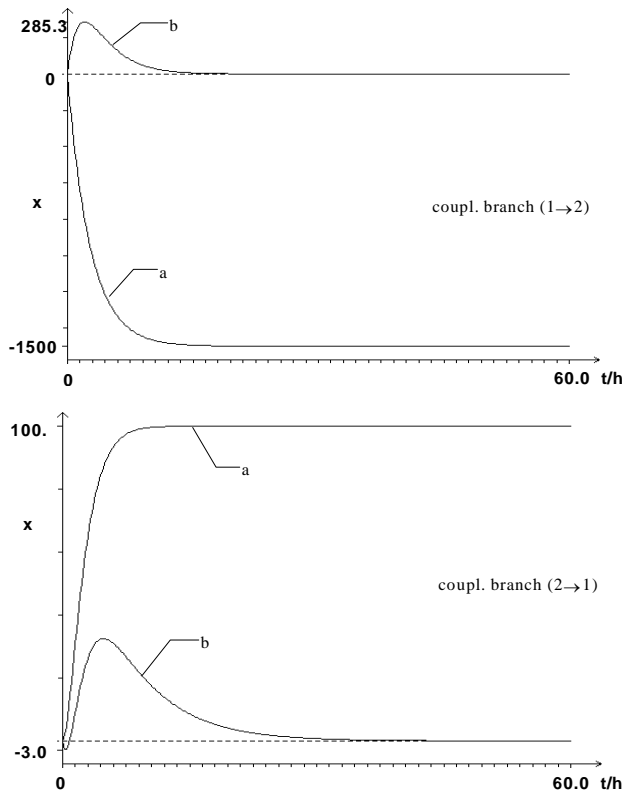Figure 3.1: Step response of the main branches I and II (a) without; and (b) with stationary decoupling.

Figure 3.2: Step response of the coupling branches (a) without; and (b) with stationary decoupling.

state decoupling. In the second step the two PI-controllers are designed for each of the two decoupled main paths of the process. The whole controller block can be regarded as multivariable PI-controller with four PI-controllers applying block transformation technique.

Design of the decoupling block

The decoupling block is designed for steady state decoupling so that there is no influence from the decoupled process input v_1 to output c_2 and from input v_2 to output c_1. From this we easily obtain through the steady state conditions for $s \to 0$:

$$
\begin{aligned}
G_{12}(0) + E_{12}G_{22}(0) &= 0 \\
G_{21}(0) + E_{21}G_{11}(0) &= 0
\end{aligned}
\tag{3}
$$

the values of the proportional decoupling block as:

$$
E_{12} = -\frac{G_{12}(0)}{G_{22}(0)} = 4.63 \quad \text{and} \quad E_{21} = -\frac{G_{21}(0)}{G_{11}(0)} = 0.082
\tag{4}
$$

Cross-over from branch II to branch I is rather small, resulting in a small decoupling coefficient E_{21}.

The input variables of the decoupled process now are v_1 and v_2, which control the two resulting main paths of the process. The transfer functions of the resulting main paths are given by:

$$
\begin{aligned}
G_{1m}(s) &= G_{11}(s) + E_{12}G_{21}(s) \\
G_{2m}(s) &= G_{22}(s) + E_{21}G_{12}(s)
\end{aligned}
\tag{5}
$$

The parallel connections introduced by the decoupling blocks cause zeros in the left-half s-plane of the transfer functions:

$$
G_{1m}(s) = -757\frac{1+0.6205\,s+2.901s^2}{1+8.8s+18.27\,s^2+10.98s^3}
$$

$$
G_{2m}(s) = 201\frac{1+3.373s}{1+4.3s+4.32s^2}
\tag{6}
$$

The step responses of the main and cross-over branches are given in Figures 3.1(b) and 3.2(b).

Due to the stationary decoupling there will be a dynamic cross-over between the circuits. The controller design will be carried out neglecting this fact. The final design will prove whether this will be of significance. Of course a dynamic decoupling can be introduced, but in many cases the dynamic decoupling blocks have to be realised by lead-blocks and introduce additional noise into the control loop. The gain of the transfer functions for the main paths with stationary decoupling is shown in Figure 4.1(a) and 4.2(a).
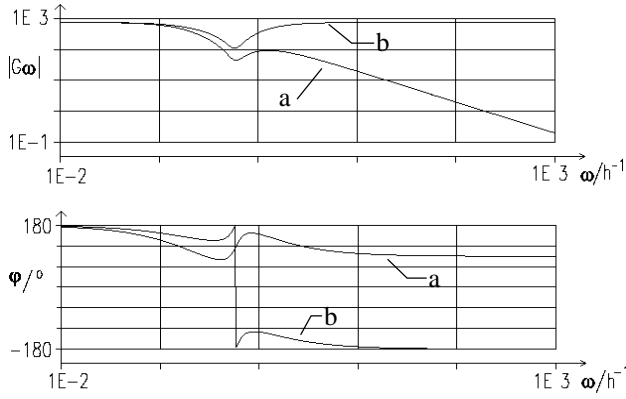
Figure 4.1: Transfer function of (a) the main path I of the decoupled process; (b) with correcting filter for maximum bandwidth.
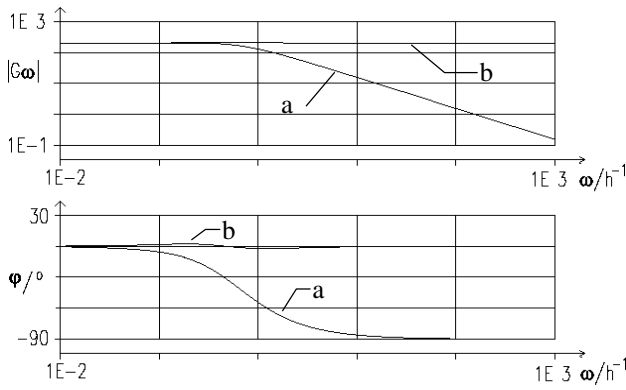

Figure 4.2: Transfer function of (a) the main path II of the decoupled process; (b) with correcting filter for maximum bandwidth.

Design of the PI-controllers [3][5-7]

In the second step the two PI-controllers for the main paths of the stationary decoupled process are designed. During the design procedure the PI-controller is regarded as a cascade of an I-controller and a correcting lead-filter (PD-filter):

$$G_{c11} = K_{P1}\left(1 + \frac{1}{sT_{r1}}\right) = \frac{K_{IC1}}{s}\left(1 + sT_{r1}\right)$$

$$G_{c22} = K_{P2}\left(1 + \frac{1}{sT_{r2}}\right) = \frac{K_{IC1}}{s}\left(1 + sT_{r2}\right) \qquad (7)$$

Design of the correcting lead-filter

We define a resulting plant as a series connection of a correcting PD-filter and a main branch of the decoupled process which is controlled by an I-controller. The lead filter is to be designed for maximum bandwidth of the resulting process. From the resulting transfer functions of the main paths:

$$\tilde{G}_{11}(s) = K_{11}\frac{\left(1 + sT_{a1} + s^2T_{b1}^2\right)\left(1 + sT_{r1}\right)}{1 + sT_{11} + s^2T_{21}^2 + s^3T_{31}^3}$$

$$\tilde{G}_{22}(s) = K_{22}\frac{\left(1 + sT_{a2}\right)\left(1 + sT_{r2}\right)}{1 + sT_{12} + s^2T_{22}^2} \qquad (8)$$

we find the high-frequency approximation:

$$\tilde{G}_{11}(\infty) = K_{11}\frac{T_{b1}^2 T_{r1}}{T_{31}^3}$$

$$\tilde{G}_{22}(\infty) = K_{22}\frac{T_{a2} T_{r2}}{T_{22}^2} \qquad (9)$$

which means that for high frequencies purely proportional behaviour is obtained for the resulting processes. For maximum bandwidth we demand that low and high frequency gain are identical. From this we find the time constants of the correcting filter as:

$$T_{r1} = \frac{T_{31}^3}{T_{b1}^2} = 3.785\,h \quad \text{and} \quad T_{r2} = \frac{T_{22}^2}{T_{a2}} = 1.281\,h \qquad (10)$$

Figures 4.1(b) and 4.2(b) show the gain transfer functions of the resulting main paths with correcting filters. The lead-filters have increased the gain for high frequencies. It can be clearly seen that the low and high frequency gains for both resulting main paths are now identical. For the main path I there is a distinct notch in the medium frequency range. For main path II only a slight increase in gain is found in the medium frequency range. If the high frequency approximation only can be made by a lag system the procedure is quite similar. Two examples are given later in the paper.

Design of the I-controller

Because of the mainly proportional character of the resulting paths of the process in the main branches, the design of the I-controller turns out to be rather simple. The transfer function for set point control $G_{SP}(s)$ can be approximated by a first order system where the time constant is determined by the integral action factor K_{IC}:

$$G_{SP1}(s) = \frac{1}{1 + s\tau_1} \qquad \text{where} \qquad \tau_1 = \frac{1}{K_{11}K_{IC1}}$$

$$(11)$$

$$G_{SP2}(s) = \frac{1}{1 + s\tau_2} \qquad \qquad \tau_2 = \frac{1}{K_{22}K_{IC2}}$$

Assuming that steady state conditions are reached at $5\tau_i$, the integral action factor K_{ICi} can be designed for

a desired settling time by the time constant of the controlled process $\tau = t_{Si}/5$:

$$K_{ICi} = \frac{1}{K_{ii}\tau_i} = \frac{5}{K_{ii} t_{Si}} \qquad (12)$$

Using the relation $K_{Pi} = K_{ICi}T_{ri}$, we find the proportional gains of the controllers for a proposed settling time $t_{S1} = t_{S2} = 0.125h$:

$$K_{P1} = \frac{5 T_{r1}}{K_{11} t_{S1}} = -0.20 \text{ and } K_{P2} = \frac{5 T_{r2}}{K_{22} t_{S2}} = 0.255 \quad (13)$$

Simulation results

Figure 5.1 and Figure 5.2 show the step response of the control circuit to a simultaneous change of the disturbances $\Delta D_1 = 1$, $\Delta D_2 = -1$ and $\Delta D_1 = 0$, $\Delta D_2 = -1$ for the above design. A change in flow rate or concentration of $\pm 20\%$ is equivalent to a change of the normalised disturbance signals $\Delta D_i = \pm 1$.

There is good disturbance rejection with fast response to changes in feed flow and concentration. The deviations in temperature are less than 1K within 0.5 hour as demanded in that project. Without control a change of 20% ($\Delta D_i = \pm 1$) of the feed flow or concentration causes a temperature change of $\pm 10K$.

In order to check performance and stability of the design, the bode-diagrams of the open loop-systems of circuit I and II are given in Figure 6. There is a phase margin of more than 95° showing that the design is very robust to parameter variations.

A FLUID MIXING PROCESS AS AN EXAMPLE FOR A MULTIVARIABLE CONTROL SYSTEM

The second example shows how multivariable control systems with a time delay (dead-time) can be designed using dynamic decoupling.

Two flows q_1 and q_2 of different temperatures ϑ_1 and ϑ_2 are being mixed in a volume V_0 (Figure 7). The temperature ϑ_0 and flow rate q_0 of the output flow are to be controlled independently. The mixing process can be described by the inner part of the block diagram in Figure 8.

The dynamics of the temperature plant are determined by the time constant of the flow mixing process and the different time delays caused by the propagation time in the tubes of the supply flows q_1 and q_2. The flow process can be considered as proportional. Additional time lag is caused by the flow valves and the sensors, which can be treated as elements
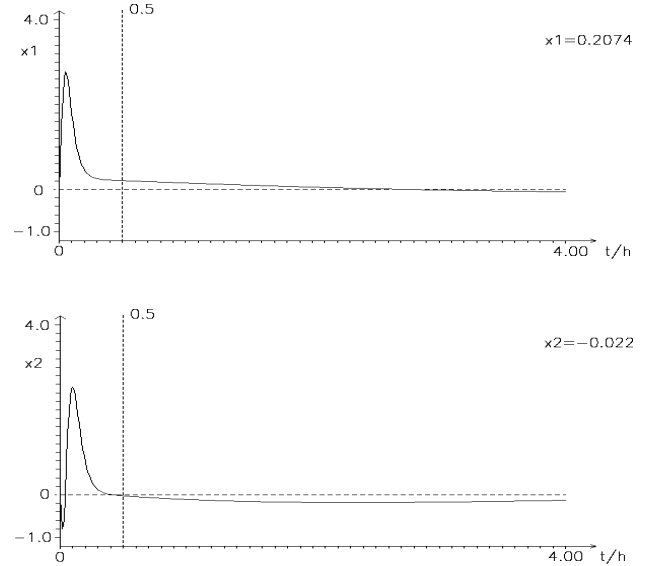
Figure 5.1: Disturbance rejection of the multivariable control circuit to sudden change of the disturbances $\Delta D_1 = 1$, $\Delta D_2 = -1$ at the process outputs.
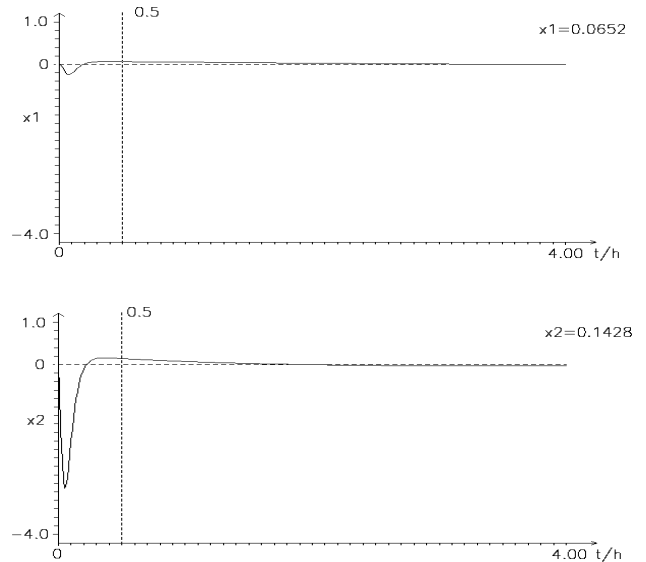
Figure 5.2: Disturbance rejection of the multivariable control circuit to sudden change of the disturbances $\Delta D_1 = 0$, $\Delta D_2 = -1$ at the process outputs.
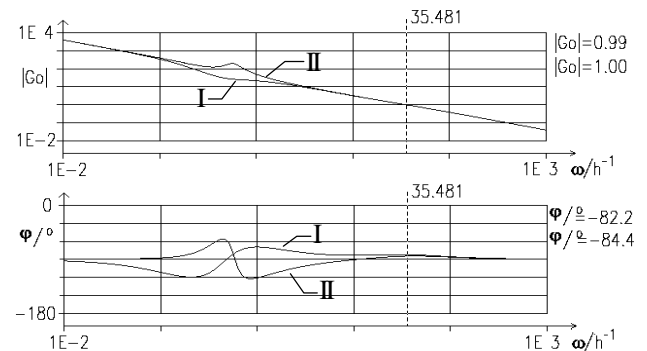
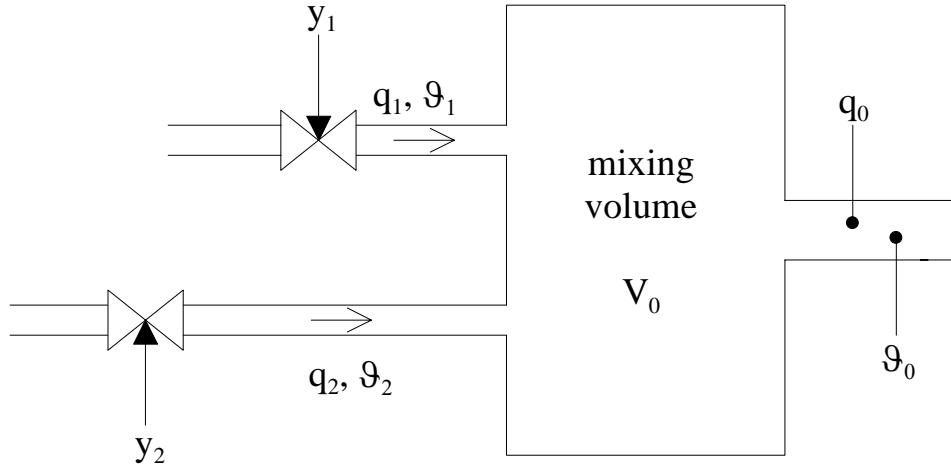Figure 6: Bode-diagram for the open loop control circuits I and II.
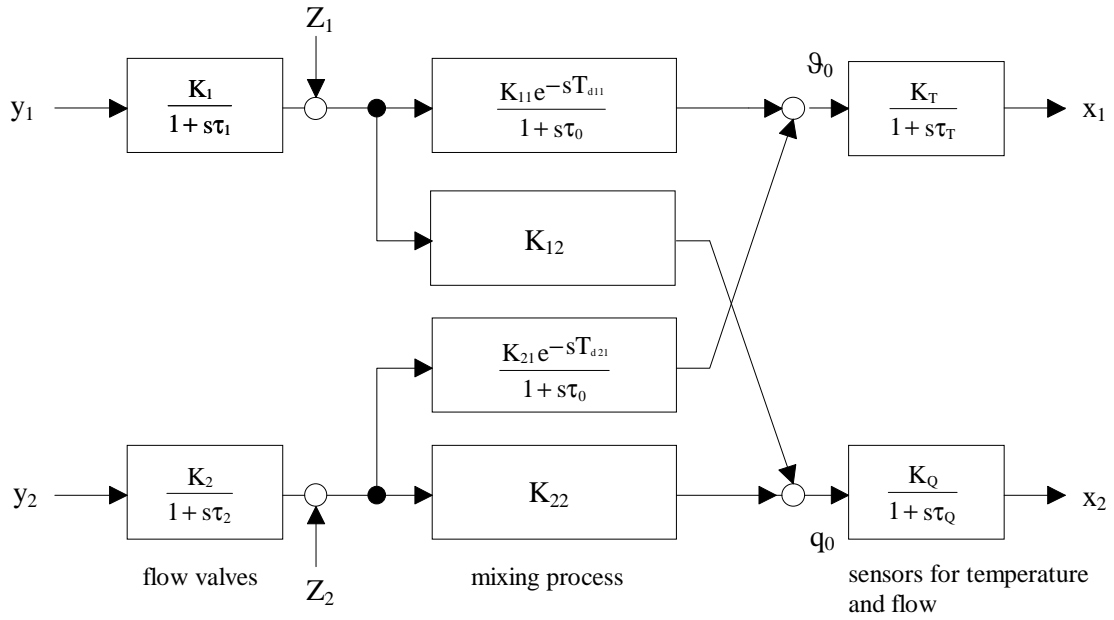
Figure 7: Flow mixing process.

Figure 8: Block diagram of the flow mixing process.

Table 1: Characteristics of the mixing process including valves and sensors.

flow valves	mixing process	sensors
$K_1 = 0.2 \dfrac{l/s}{V}$ $\tau_1 = 0.3s$	$K_{11} = 20 \dfrac{^0C}{l/s}$, $\tau_0 = 10s$, $T_{d11} = 3.6s$ $K_{12} = 1$ $K_{21} = -\dfrac{30^0C}{l/s}$, $\tau_0 = 10s$, $T_{d11} = 5.0s$	$K_T = 0.1 \dfrac{V}{^0C}$ $\tau_T = 2s$
$K_2 = 0.2 \dfrac{l/s}{V}$ $\tau_2 = 0.3s$	$K_{22} = 1$	$K_Q = 5 \dfrac{V}{l/s}$ $\tau_Q = 0.2s$

with first order lag. In detail the characteristics of the whole process, including valves and sensors, are given in Table 1.

From this we find the transfer functions of the whole process (Figure 8):

$$G_{11}(s) = \frac{0.4\,e^{-3.6s}}{(1+0.3s)(1+2s)(1+10s)}$$

$$G_{12}(s) = \frac{1}{(1+0.2s)(1+0.3s)} \qquad (14)$$

$$G_{21}(s) = \frac{-0.6\,e^{-5s}}{(1+0.3s)(1+2s)(1+10s)}$$

$$G_{22}(s) = \frac{1}{(1+0.2s)(1+0.3s)}$$

All time constants are given in seconds.

The step responses of the main and cross-over branches are shown in Figures 9(a) and 10(a). The controller design is now performed similar to the first example. Refer to Figure 2 for a complete block diagram of the control circuit.

Design of the decoupling block

The decoupling block will be designed for dynamic conditions:

$$E_{12}(s) = -\frac{G_{12}(s)}{G_{22}(s)} = -1 \qquad (15)$$

$$E_{21}(s) = -\frac{G_{21}(s)}{G_{11}(s)} = 1.5\,e^{-1.4s} \approx \frac{1.5}{1+1.4s+0.98s^2} \qquad (16)$$

Block E_{12} turns out to be purely proportional, whereas block E_{21} needs a delay characteristic, which is approximated by a second order lag filter using Taylor series expansion.

Figure 11 shows the result of cross-coupling from branch 2 to branch 1 for an approximately dynamic decoupling compared to a purely stationary decoupling applying a step change to input v_2. For stationary decoupling there is a significant influence from the (lower) flow control branch to the (upper) temperature control branch. In the case of dynamic decoupling there is only a negligible short time deviation.

The PI-controller block is now designed for the two resulting main paths of the decoupled process neglecting the effects of cross-coupling. The next step therefore is to determine the resulting transfer functions of the two main paths for temperature and flow control.
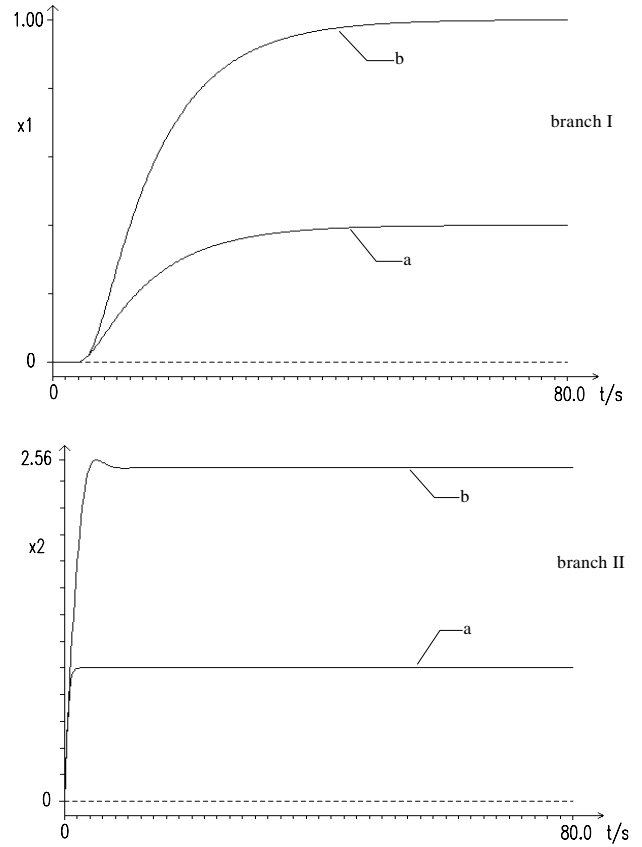

Figure 9: Step responses of the main branches I and II, (a) without; and (b) with dynamic decoupling.
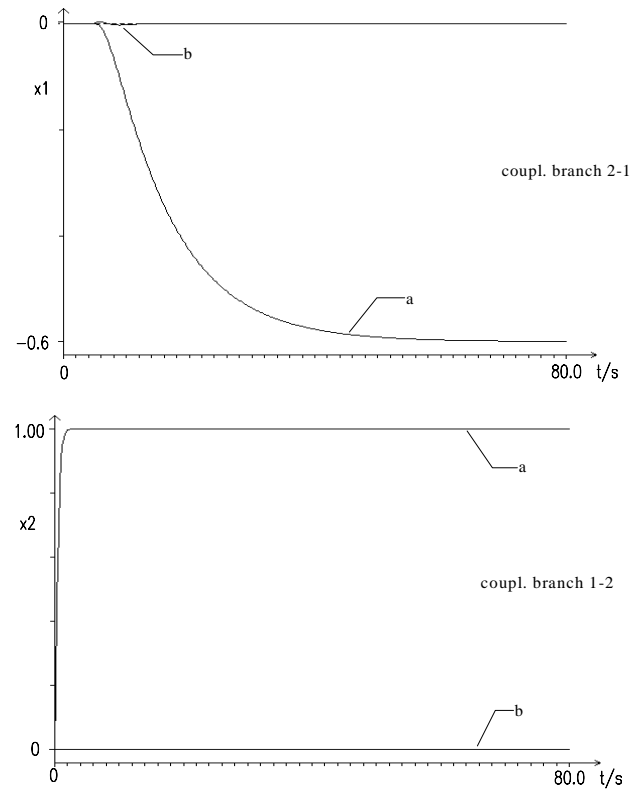

Figure 10: Step responses of the coupling branches (a) without; and (b) with dynamic decoupling.
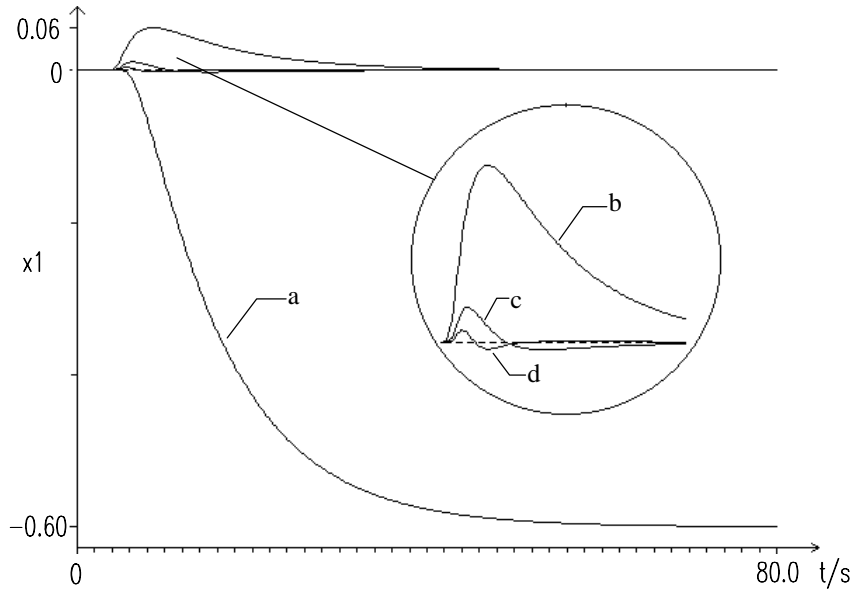
Figure 11: (a) Step response of the coupling branch 2-1 (v_2 to x_1) and with decoupling; (b) pure stationary; (c) first order; (d) second order.

Resulting main path I for temperature control

The decoupling block E_{12} causes a paralleling of block G_{11} and G_{21}:

$$G_{1m}(s) = G_{11}(s) + E_{12}(s)G_{21}(s)$$

$$= \frac{0.4\,e^{-3.6s} + 0.6\,e^{-5s}}{(1+0.3s)(1+10s)(1+2s)} \tag{17}$$

By approximation of the delay terms through second order transfer functions we obtain a transfer function:

$$G_{1m}(s) \approx$$
$$\frac{1+4.16s+8.89s^2}{(1+0.3s)(1+2s)(1+10s)(1+3.6s+6.48s^2)(1+5s+12.5s^2)} \tag{18}$$

with a second order lead term in the denominator, which again can be approximated by applying Taylor series expansion for the denominator term using:

$$1 + sT_a + s^2T_b^2 \approx \frac{1}{1 - sT_a + s^2\left(T_a^2 - T_b^2\right)} \tag{19}$$

The low frequency approximation of the main branch I for temperature control results in:

$$G_{1m}(s) \approx \frac{1}{1+16.74s+87.83s^2} \tag{20}$$

Resulting main path II for output flow control

The decoupling block E_{21} causes a paralleling of block G_{22} and G_{12}:

$$G_{2m}(s) = G_{22}(s) + E_{21}(s)G_{12}(s)$$

$$= 2.5\frac{1+0.56s+0.392s^2}{(1+0.2s)(1+0.3s)(1+1.4s+0.98s^2)} \tag{21}$$

$$\approx \frac{2.5}{1+1.34s+0.60s^2}$$

The denominator term is treated in the same way as for branch I.

The time constants of the denominator term are much smaller than those of the same order in the nominator term, allowing approximation by a second order lag using Taylor series expansion. The low frequency behaviour of the parallel plant is used for the design of the PI-controller.

Design of the PI-controller block [3][5-7]

The two PI-controllers for the decoupled process can now be designed applying the criterion of cascaded damping ratios using the second order approximations of the plant according:

$$G_p(s) \approx \frac{K}{1+sT_1 + s^2T_2^2} \tag{22}$$

During the design procedure the PI-controller is regarded as a cascade of an I-controller and a correcting lead-filter (PD-filter).

For the sharp design the controller parameters follow as:

$$T_r = T_1 - \frac{T_2^2}{T_1} \qquad K_P = \frac{0.375}{K}\frac{T_r}{T_1 - T_r} \tag{23}$$

The reset time T_r is evaluated for maximum bandwidth of the series connection of the main branch of the decoupled process and the correcting lead-filter at an equivalent damping ratio $d_1 = 0.5$. The I-controller is designed for an equivalent damping ratio of $d_0 = \sqrt{2/3}$ for the closed loop.

From this the parameters of the controllers follow as:

$$T_{r1} = 11.50s \qquad T_{r2} = 0.89s$$

$$K_{P1} = 0.82 \qquad K_{P2} = 0.30$$

Figures 12 and 13 show the frequency transfer functions of the resulting main paths with correcting filters. In both cases it can be seen that the lead filters are properly designed and significantly increase the bandwidth.

In order to check stability the Bode-diagrams in Figure 14 show the open loop transfer functions of the two control circuits. Phase and amplitude margin are as follows:

Temperature control loop I: $\qquad \Phi_m \approx 65°$, $A_m = 3.4$

Flow control loop: $\qquad \Phi_m \approx 64°$, $A_m = \infty$

These values lie within the recommendation for a robust control circuit design.

Simulation results

Figure 15(a) shows the time response of the control circuit to a simultaneous change of both references for temperature and flow. There is no interference between the two control circuits as the result of the dynamic decoupling. Due to the time lag caused by the mixing process, the temperature control circuit is significantly slower than the flow control circuit, which is mainly determined by the dynamics of the flow valves and the flow sensor.

The same Figure 15(b) shows the disturbance rejection for a 10% step change in flow of $z_2 = 0.05$ l/s at $t_1 = 20s$ and $z_1 = 0.05$ l/s at $t_2 = 60s$. Because the disturbances occur at the process input, the decoupling block will not operate instantly and therefore the effect of cross-coupling is much stronger than for reference control. Clearly the problem of large delay-times can be observed. The disturbances are transmitted nearly in full strength until the controllers get into action. After that the disturbance rejection is carried out according to the dynamics of the two control branches. See Table 2 for operating conditions of the flow mixing process.

HANDLING THE PROBLEM OF PARALLEL EFFECTS IN DECOUPLED BRANCHES

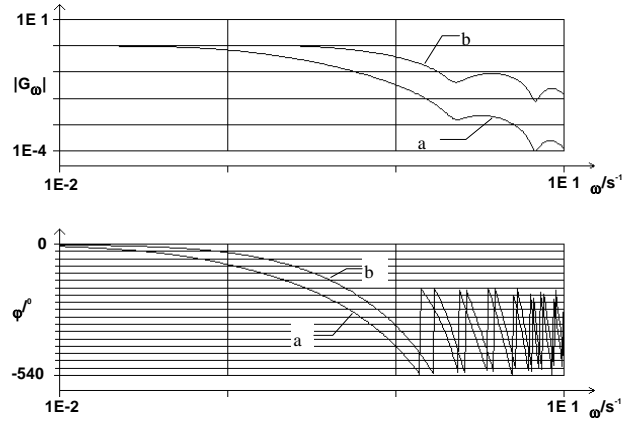By introducing a decoupling block into a multi-vari-

Figure 12: Transfer function of (a) the main path I of the decoupled process; and (b) with correcting filter for maximum bandwidth.
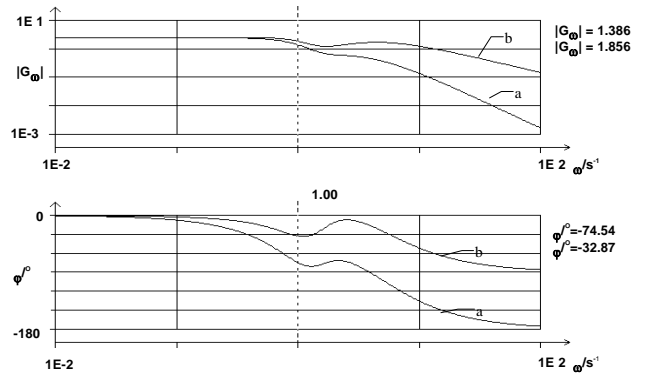

Figure 13: Transfer function of (a) the main path II of the decoupled process; and (b) with correcting filter for maximum bandwidth.
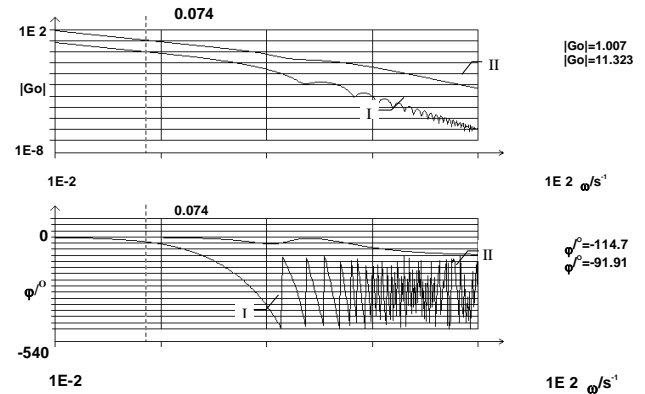

Figure 14: Bode-diagram for the open loop control circuit I and II.

able plant a paralleling of the paths of the original plant is caused. Depending on superposition in the same or opposite sense, the transfer functions can show zeros in the left-half or right-half s-plane. Left-half s-plane zeros can result in a steep rise of the step response followed by creeping to the steady state. This may also be joined by a distinct over-
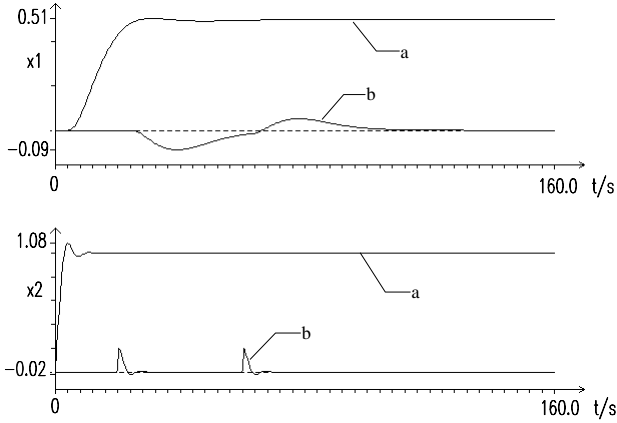
Figure 15: Response of the control circuit to (a) simultaneous command step of r_1 and r_2 followed by (b) disturbance step changes d_2 at $t = 20s$ and d_1 at $t = 60s$.

shoot of the step response. Right-half s-plane zeros give rise to responses that initially go to the opposite direction of the steady-state response. The following two examples shall demonstrate how to treat these effects.

SUPERPOSITION IN THE SAME SENSE (ZEROS IN THE LEFT-HALF S-PLANE)

Example 1

A PI-controller for a transfer function of a plant with parallel effects, including the correcting filter according to equation (24), is to be designed:

$$\tilde{G}(s) = \frac{K(1 + sT_a)(1 + sT_r)}{1 + T_1 s + T_2^2 s^2 + T_3^3 s^3} \qquad \begin{aligned} T_a &= 40s \\ T_1 &= 70s \\ T_2^2 &= 732s^2 \\ T_3^3 &= 2088s^3 \\ K &= 1 \end{aligned} \qquad (24)$$

The gain transfer function of the plant without correcting PD-filter shows a slow decrease in the medium and a fast decrease in the high frequency range. A high frequency approximation of the resultant plant shows first order lag:

$$\tilde{G}(s) \approx K \frac{T_a T_r}{T_2^2} \frac{1}{1 + sT_3^3 / T_2^2} \qquad (25)$$

In order to achieve maximum bandwidth the high frequency gain has to be equal to the low frequency gain K. This leads to the relation for the time constant of the correcting filter which is identical to the reset time T_r of the I-controller:

$$T_r = \frac{T_2^2}{T_a} = 18.3s \qquad (26)$$

Figure 16 demonstrates the effect of the correcting filter. The bandwidth is significantly increased compared to that of the original plant. After a certain sagging of the gain in the medium range a maximum is found that is about 12% higher than the desired value of 1. According to this deviation the reset time is adjusted to $T_r = 16.32s$. The I-controller of the series connection (equation 7) is designed for a damping ratio of the closed loop $d_0 = 1/\sqrt{2}$ resp. $d_0 = \sqrt{2/3}$ using first order approximation of the resulting plant:

$$K_I = \frac{1}{4d_0^2 K \dfrac{T_3^3}{T_2^2}} \qquad (27)$$

From this we find the proportional gain and the reset time of the PI-controller:

$$K_p = K_I T_r = \frac{(0.375...0.5)T_r T_2^2}{T_3^3} = 2.14...2.86$$

$$T_r = 16.32s \qquad (28)$$

Figure 17 shows the step response of the plant with a zero in the left-half of the s-plane (a), and control circuit with PI-controller (b).

Example 2

The transfer function of the plant including the correcting filter of the PI-controller is given by:

$$\tilde{G}(s) = \frac{K(1 + T_a s + T_b^2 s^2)(1 + sT_r)}{1 + T_1 s + T_2^2 s^2 + T_3^3 s^3 + T_4^4 s^4} \qquad (29)$$

with parameters of the plant:

Table 2: Operating conditions of the flow mixing process.

Operating point	reference change	disturbance change
$\vartheta_{00} = 40 \,°C$	$\Delta\vartheta_{00} = 5 \,°C$	$\Delta q_1 = 0.05 \,l/s$
$q_{00} = 1 \,l/s$	$\Delta q_{00} = 0.2 \,l/s$	$\Delta q_2 = 0.05 \,l/s$

$K = 2, \quad T_a = 12.95s, \quad T_b^2 = 9.95 \ s^2$

$T_1 = 3.525s, \quad T_2^2 = 3.5875s^2, \quad T_3^3 = 1.0875s^3,$

$T_4^4 = 0.025s^4$

The step response of the plant in Figure 18 shows a large overshoot because T_a is significantly higher than T_1.

The gain transfer function in Figure 19(a) shows an increase in the medium frequency range and a decrease for higher frequencies. In order to obtain maximum bandwidth the correcting lead filter has to be designed so that the gains of the resulting plant in the medium and high frequency range are equal. This leads to the relation:

$$\frac{T_b^2 T_r}{T_3^3} = \frac{T_b^2 + T_a T_r}{T_2^2} \tag{30}$$

high   medium
frequency   frequency
gain   gain

From this the reset time of the PI-controller results in:

$$T_r = \frac{1}{\dfrac{T_2^2}{T_3^3} - \dfrac{T_a}{T_b^2}} = 0.50s \tag{31}$$

The gain transfer of the resulting plant with lead filter shows a remarkable increase in bandwidth in the high frequency range. The I-controller is designed taking the high frequency approximation of the resulting plant:

$$\tilde{G}(s) \approx K \frac{T_b^2 T_r}{T_3^3} \frac{1}{1 + s\dfrac{T_4^4}{T_3^3}} = \frac{K^*}{1 + sT_1^*} \tag{32}$$

for a damping ratio of the closed loop $d_0 = 1/\sqrt{2}$ resp. $d_0 = \sqrt{2/3}$. This leads to an integral action factor of the I-controller:

$$K_I = \frac{1}{4d_0^2 K^* T_1^*} = \frac{(0.375...05)}{K} \frac{\left(T_3^3\right)^2}{T_r T_b^2 T_4^4} \tag{33}$$

$= 1.783..2.377 s^{-1}$

The proportional gain of the PI-controller follows as:

$$K_P = K_I T_r = \frac{(0.375...0.5)}{K} \frac{\left(T_3^3\right)^2}{T_b^2 T_4^4} = 0.891...1.19 \tag{34}$$
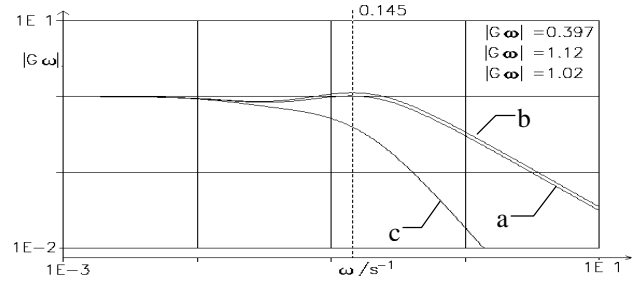
Figure 20 shows the response of the control cir-

Figure 16: Gain transfer function of the plant with zero in the left-half of the s-plan (a) without; (b) with correcting filter $T_r=18.3s$; and (c) adjusted $T_r=16.32s$.
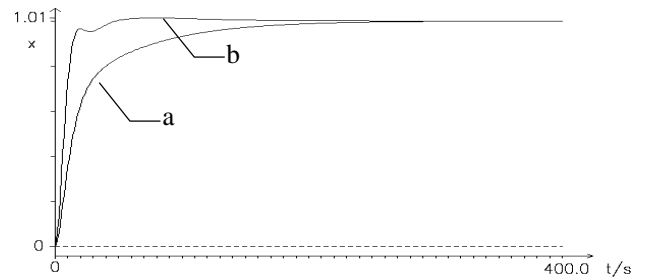

Figure 17: Step response of (a) the plant with zero in the left-half s-plane; and (b) control circuit with PI-controller.
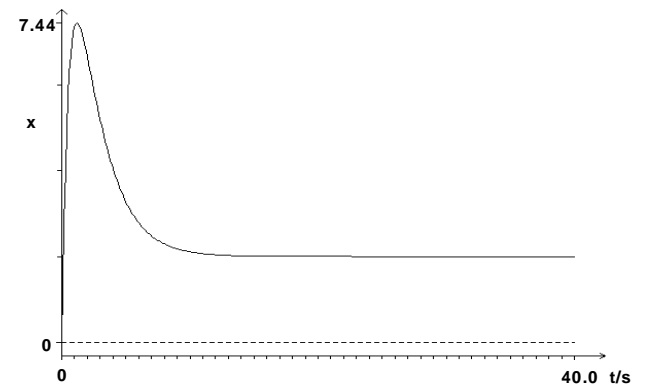

Figure 18: Step response of the plant with unique overshoot (two zeros in the left half of the s-plane).
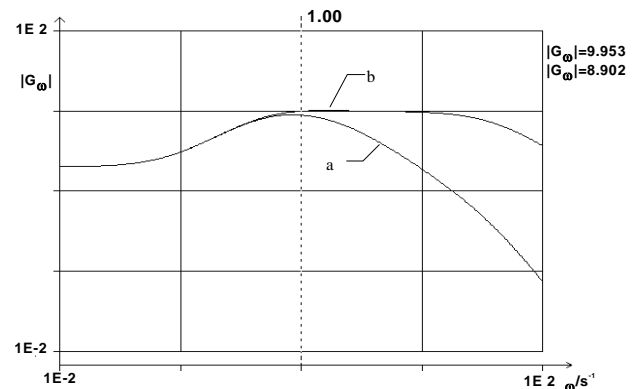

Figure 19: Gain transfer function of the plant with zeros in the left-half of the s-plane (a) without; and (b) with correcting filter.

cuit to a step change of the reference variable and the response to a step change of the disturbance. The response is so fast that the resolution is too poor in that scale. The settling time of the process without control is roughly 10s, whereas the controlled process settles in less than 0.5s. Therefore in Figure 21 the first four seconds of the response are zoomed. The result is remarkable. Within 0.5 seconds the controlled variable is in the range of the steady state value within less than 0.1%. The control variable reacts with a sharp pulse at the beginning and then steadily increases, reaching its final value of 0.5 after nearly 40 seconds according to the steady state gain of the plant $K = 2$ as to be seen from Figure 20.

It is important that the correcting filter is determined by the high frequency behaviour of the plant, resulting in a rather small value for the reset time compared with the time constants of the process in equation (29). The explanation is quite simple. The fast rise in the time domain is equivalent to the high frequency behaviour in the frequency range. For any changes in the control circuit the controller reacts in the first moment according to the rise of the plant given by its time response in Figure 18. This is the reason why the controlled variable reaches the steady state value in such a short time, whereas the control variable after the initial pulse is steadily increasing from its lowest value, which corresponds to the high frequency gain to the highest value corresponding to the low frequency gain.

SUPERPOSITION IN THE OPPOSITE SENSE (ZEROS IN THE RIGHT-HALF S-PLANE)

Example 3

As a result of two second order systems in parallel, we assume a fourth-order transfer function of a plant with a zero each in the left and right-half s-plane:

$$G(s) = \frac{1 - 1.5s - 2.5s^2}{1 + 4.5s + 7.0s^2 + 4.5s^3 + 1.0s^4}$$

$$\approx \frac{1}{1 + 6.0s + 18.5s^2} \quad \text{low frequency response (35)}$$

The step response in Figure 22(a) shows a significant undershoot of about 37%. The influence of right-plane
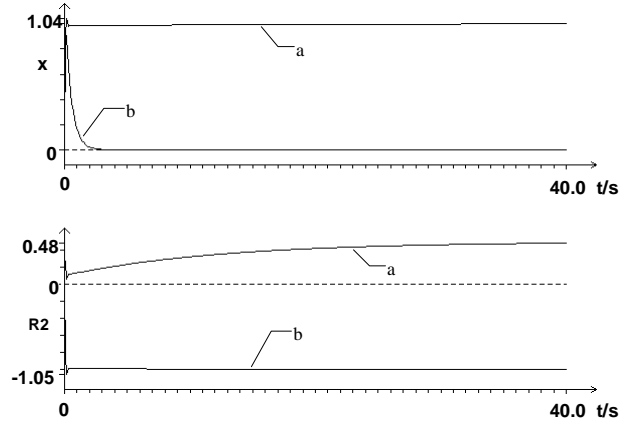
Figure 20: Step response of the control circuit for (a) reference control; and (b) disturbance rejection, first: controlled variable, second: control variable. Recording time 40s.
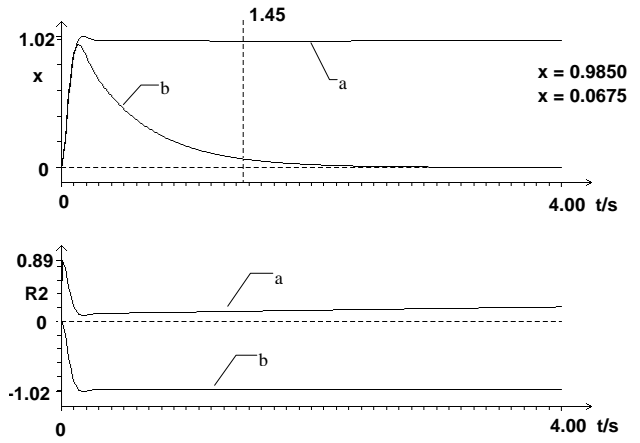
Figure 21: Zoom of the first four seconds. Step response of the control circuit for (a) reference control; and (b) disturbance rejection, first: controlled variable, second: control variable.

zeros can be approximated by left-plane poles using Taylor-series expansion for a low frequency approximation of the plant. From this a PI-controller can be designed according to the principle of cascaded damping ratios:

$$T_r = T_1 - \frac{T_2^2}{T_1} = 2.92s$$

$$K_P = \frac{T_r}{4d_0^2 (T_1 - T_r)} = 0.355 \ldots 0.473 \quad (36)$$

Figure 22(b) and (c) show the simulation results for PI-control. Through variation for the damping factor between $d_0 = 1/\sqrt{2}$ and $d_0 = \sqrt{2/3}$ a compromise may be chosen between the under and overshoot of the controlled variable which influences the settling time of the control circuit.
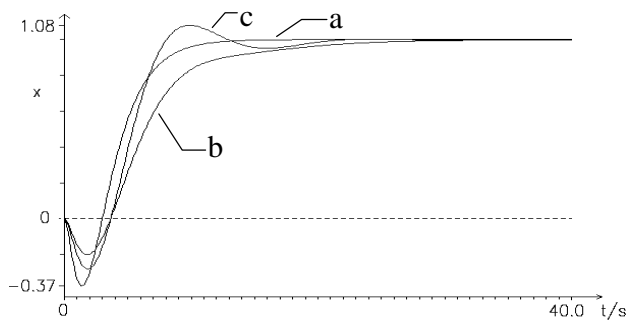
Figure 22: Step response of (a) the plant with a zero in left-half s-plane; (b) control circuit with PI-controller K_p=0.355, T_r=2.92s; and (c) K_p=0.473, T_r=2.92.

CONCLUDING REMARKS

Due to the importance of multivariable control systems, basic control engineering education should cover this area. For this we need transparent design methods that can be taught without an unnecessary bulk of mathematics. Then we can expect that not only engineers with a special education in control theory will be able to solve such problems. This will save costs and improve the quality of products. The method presented in this paper has been evaluated during a project titled *Quality in Engineering Education*, which was supported by the Ministry for Science and Research and Development of Northrhine-Westfalia. It will be integrated into the basic lectures of control engineering in the Department of Information Technology at the FH Köln during 1998/99.

REFERENCES

1. Raisch, J., *Mehrgrößenregelung im Frequenz-bereich.* München, Wien: R. Oldenburg Verlag (1994).

2. Raisch, J., Lang, L. and Groebel, M., Loop shaping controller design for a binary distillation column. *Proc. International Conf. on Control*, Edinburgh, 1271-1276 (1991).

3. Schaedel, H.M., *Entwurf von parameter-optimierten Reglern nach dem Kriterium der gestuften Dämpfung.* FH Köln (1995).

4. Schaedel, H.M., Design of a multivariable controller for a binary distillation column. Internal report (in German) 96/1, FH Köln (1996).

5. Schaedel, H.M. and Hilger, F.J., New methods and CAE-tools for improving basic control engineering education. *Proc. 3rd East-West Cong. on Engng. Educ.*, Gdynia, Poland, 176-188 (1996).

6. Schaedel, H.M., A new method of direct PID controller design based on the principle of cascaded damping ratios. *Proc. European Control Conf.*, Brussels, paper WE-A-H4 (1997).

7. Schaedel, H.M., Direkter Entwurf parameter-optimierter Regler nach dem Kriterium der gestuften Dämpfung. *Proc. Jahrestagung der Deutschen Forschungsvereinigung für Meß-Regelungs-und Systemtechnik*, Bremen, Germany, Forschungsbericht 95-1, 117-153 (1995).

8. Schaedel, H.M., *Entwurf von Mehrgrößen-systemen.* FH Köln (1999).

BIOGRAPHIES

Herbert M. Schaedel is currently a professor of Control Engineering in the Department of Information Technology, the University of Applied Sciences Köln, Federal Republic of Germany. He obtained his degree, a Dipl-Ing in Electrical Engineering in 1964, and his doctorate in 1968. He has acquired industrial experience in electronic precision measurement techniques and in control engineering and is member of two commissions of the German Association of Electrical Engineers.

In 1971 he began lecturing control engineering and digital networks at the Fachhochschule Köln, and was appointed professor in 1972. His main interest in the years between 1971-1980 was in fluidic network design. He has published more than thirty journal and conference articles and one book on this subject.

Since 1980 his main interest has been in digital control and signal processing, and, since 1986, in CAE-tools and practical design methods for engineering education and industrial application in control engineering. He has written about ten articles and conference papers concerning his new field of interest. Since 1992 he has been head of the research group *CAE and fuzzy-technology in control engineering*.
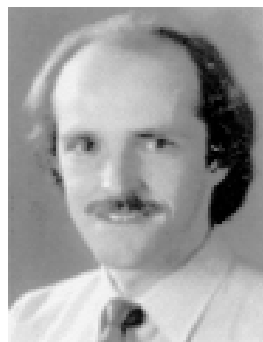
Rainer Bartz is currently a professor in Control Engineering in the Department of Information Technology at FH Köln, University of Applied Sciences, Federal Republic of Germany.

He studied at RWTH Aachen and received his Diplom degree from the Faculty of Electrical Engi-

neering in 1983 on traffic analysis based on inductive measurements. He then became project engineer for measurement equipment development in a company that mainly focuses on research and development of combustion engines. In 1989 he received his PhD degree from the Faculty of Mechanical Engineering at RWTH Aachen for his studies on applying pattern recognition methods to improve the knock-detection in spark ignited engines. From 1989 to 1997 he was Head of Development, responsible for hardware and software of measurement and control equipment and for co-operation with a US company.

Rainer Bartz is member of the ASAM, a recently founded European organisation working on standards for measurement and automation systems. He became a professor in 1997. His main areas of interest are disseminating the new PID design methods developed by Professor Schaedel as well as establishing a field-bus laboratory to introduce this rather new technical topic into education and research.